Luminescent Transparent Wood

*Yuanyuan Li, Shun Yu, Jonathan G. C. Veinot, Jan Linnros, Lars Berglund, and Ilya Sychugov**

Functional light conversion layers containing active fluorescent materials are necessary components in many devices. The most straightforward example would be the common white light-emitting diode (LED), where blue emission from a GaN-based diode is partially converted to red and green emission using a phosphor-rich layer. Most commercial devices rely on rare-earth-based phosphors,[1] however quantum dots (QDs) have also been considered.[2] These nanosized light emitters are usually dispersed in homogeneous silica[3] or polymer[4,5] layers in close proximity to the excitation LED. Thus their size is relatively small, and the concentration of fluorescent centers high. Typically, they are combined with an additional passive diffuser component to minimize the influences of viewing angle and to achieve uniform illumination, such as using a patterned structure,[6] porous layers,[7,8] or films with embedded microparticles[9,10]

So far, white LEDs have been thought of as distinct localized illumination sources, which are not part of the constructions or materials they illuminate. In this letter we present the preparation of a conversion layer realized by the virtue of the natural porous wood structure of the newly developed transparent wood material.[11] In contrast to thin layers of transparent nanocellulose paper,[12] this delignified wood represents a 3D porous bulk structure suitable as reinforcement in load-bearing components. Matching the refractive indices of the pore-filling polymer and the cellulose fibers ensures optical transparency.[11,13,14] Here the pore-filling monomer methyl methacrylate (MMA) was enriched with luminescent QDs before embedding it into the cellulose fiber network for subsequent polymerization. We show that QDs reveal no signs of optical degradation upon this transition, where different nanocrystal materials were tested. Under blue/UV excitation the resulting $2 \times 2 \times 0.2$ cm slabs exhibited diffused red and green luminescence arising from the embedded Si and CdSe QDs, respectively. Structures containing Si QDs offer a unique opportunity to evaluate scattering losses because the optically active Si QDs have negligible reabsorption at the emission wavelength.[15] The scattering strength of the luminescence was found to be dependent on the wood fiber direction, consistent with the original wood structure being preserved. High scattering values (i.e., up to ≈ 10 dB cm^{-1}) indicate strong suppression of the total internal reflection required for emitted light propagation. This luminescent transparent wood nanocomposite offers interesting possibilities for applications, which can benefit from its unique structural and optical properties. Examples would be furniture for general lighting or luminescent solar concentrators for building integration,[16–19] where the proven mechanical strength of this transparent wood[11] is a clear advantage. The nontoxicity and material abundance of Si QDs further enables sustainable and large scale manufacturing of this new luminescent material.

Silicon QDs were synthesized upon processing of hydrogen silsesquioxane by thermal annealing.[20] The resulting nanocrystal-containing silicon oxide composites were treated with ethanolic hydrofluoric acid to extract hydride terminated nanocrystals. It was followed by surface passivation using well-established hydrosilylation procedures described elsewhere.[21,22] Toluene dispersions of the resulting alkyl-passivated Si QDs feature external photoluminescence quantum yields in the range 30%–60%.[23] Samples used here had peak positions in the red (720 nm) and near infrared (870 nm) spectral range. To demonstrate the possibility of incorporating different types of QDs commercially available CdSe/ZnS core/shell quantum dots with green emission (540 nm, Evident Technologies) were used.

The wood template was obtained by delignification of wood veneer (balsa, *Ochroma pyramidale*, purchased from Wentzels Co. Ltd, Sweden) with dimension of $2 \times 2 \times 0.2$ cm to remove the main light-absorbing component.[24] The thickness direction of the veneer is the tangential direction of the cross-section of the tree stem. Specifically, wood veneer was treated using 1 wt% of sodium chlorite ($NaClO_2$, Sigma-Aldrich) in acetate buffer solution (pH 4.6) at 80 °C. The reaction was stopped when the wood appeared almost uniformly white. The delignified samples were washed with deionized water and kept in water until further use. Prior to polymer infiltration, wood samples were dehydrated upon sequential exposure to ethanol and acetone with each solvent exchange step repeated three times. The MMA monomer was pre-polymerized before mixing with QDs. The prepolymerization was completed by heating the MMA at 75 °C for 15 min with 0.3 wt% 2,2′-azobis (2-methylpropionitrile) followed by cooling to room temperature. This process yielded a mixed solution with MMA monomers and oligomers. Subsequently, the delignified wood template was

Dr. Y. Li, Dr. S. Yu, Prof. L. Berglund
Wallenberg Wood Science Center
Department of Fibre and Polymer Technology
Chemical Science and Engineering
KTH Royal Institute of Technology
SE-100 44 Stockholm, Sweden
Prof. J. G. C. Veinot
Department of Chemistry
University of Alberta
Edmonton, Alberta T6G 2G2, Canada
Prof. J. Linnros, Prof. I. Sychugov
Materials and Nano Physics Department
ICT School
KTH Royal Institute of Technology
16440 Kista, Sweden
E-mail: ilyas@kth.se

DOI: 10.1002/adom.201600834

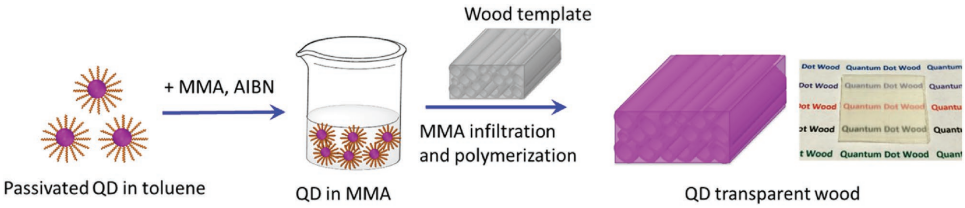

Figure 1. Left: Schematic of the preparation of quantum dot (QD) transparent wood, where 2,2′-azobis (2-methylpropionitrile) (AIBN) was applied as the initiator for MMA polymerization. Right: A photograph of a representative sample under ambient light.

fully vacuum-infiltrated with the prepolymerized MMA/QDs solution in a desiccator under house vacuum with pressure of 13 mbar. Finally, the infiltrated wood was sandwiched between two glass slides, wrapped with aluminum foil, and heated in an oven at 70 °C for 4 h in ambient atmosphere (**Figure 1**). The rightmost image in Figure 1 shows the red-emitting Si QDs containing transparent wood composite with letters beneath clearly visible under ambient light.

Absolute photoluminescence (PL) quantum yields, luminescence, and absorption spectra were measured in a home-built instrument based on an integrating sphere. The selected excitation wavelength was 440 nm (6 nm linewidth) filtered by a monochromator after a laser-driven Xe-lamp.[23] To evaluate the scattering strength, the QD luminescence was collected from the sample edge using a 10× objective lens of an inverted microscope and detected by a CCD camera. The excitation spot (≈1 mm diameter) was focused on the sample front surface from a 405 nm laser diode and scanned across it using a mirror system. For PL mapping a color camera (Zeiss, AxioCam) was used and the image was taken from the sample edge with a 100× objective lens after a long pass 635 nm filter under broad spot excitation from the 405 nm laser. For structural characterization cross-sections of QD wood samples were investigated using a field-emission scanning electron microscope (SEM, Hitachi S4800) operating at a low acceleration voltage of 1 kV and in the secondary electron collection regime. The cross-section was prepared by fracturing a freeze-dried sample after cooling in liquid nitrogen and polishing with 1–10 µm sand paper.

SEM analysis reveals that the QD-rich polymer fully infiltrates pores of the delignified wood without large cavities visible at this magnification (**Figure 2**a). To gain insight into the distribution of QDs throughout the wood template, PL mapping was performed. This imaging reveals a uniform distribution of emission centers (Figure 2b) with signal intensity varying within 10% across the image (noticeable grooves appearing in the image are the results of surface polishing).

Embedding QDs in polymer matrices can lead to deterioration of their optical properties due to particle aggregation,[25] however we have demonstrated that Si QDs encapsulated in acrylic glass retained their optical properties (i.e., peak position, quantum yield, and lifetime).[26] The fabrication procedure employed to prepare the present hybrid materials differs slightly and includes a mixing of a prepolymerized MMA with QD solution, an infiltration into the cellulose fiber network followed by a final heat treatment. To interrogate any potential impact of this synthetic approach on the QDs optical performance, we monitored the luminescence quantum yield. To reduce the measurement error related to limited absorption, a high initial concentration of QDs in toluene was used (>0.1 wt%). The initial sample of Si QDs in toluene solution showed a broad emission peak at 870 nm (particle average diameter ≈6 nm) and 35%–40% quantum yield. A QD-free wood reference sample

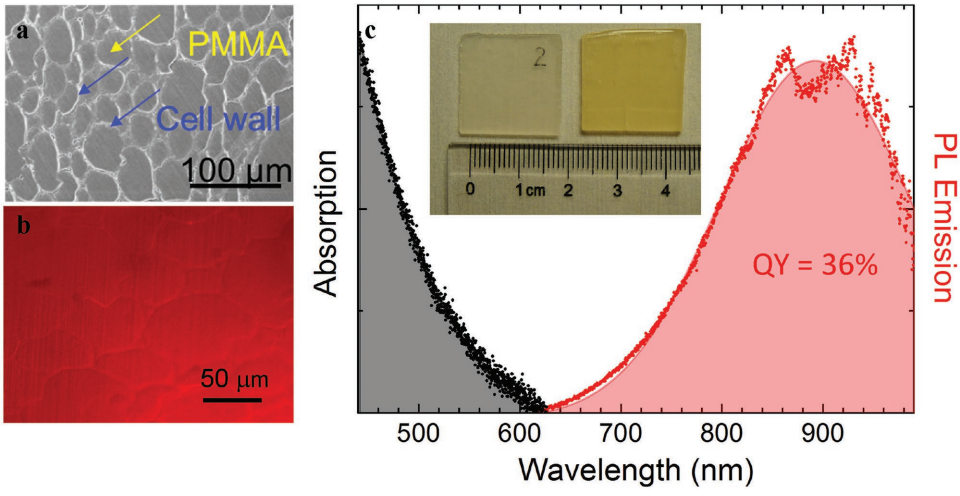

Figure 2. a) Cross-sectional SEM image of Si QDs containing transparent wood; the yellow arrow points to QD/PMMA in the pore, blue arrows point to the wood cell wall. b) Real color PL mapping of Si QDs in the sample, revealing a uniform distribution. c) Absorption and PL emission curves of the near-infrared Si QD wood (dips at 830 and 870 nm are absorption from the remaining toluene). Inset image shows the actual samples: (left) transparent wood and (right) Si QD wood prepared for QY measurements with a ruler for the actual scale.

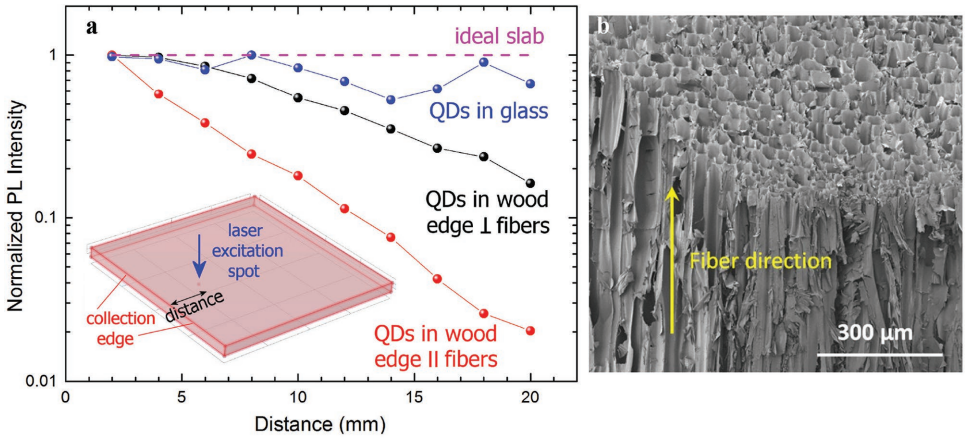

Figure 3. a) Photoluminescence of QD transparent wood collected as a function of excitation spot distance from the sample edge: parallel and perpendicular to the fiber direction (red and black), photoluminescence of QDs in glass collected as a reference (blue); b) SEM image of wood showing the preferential alignment of cells.

(left) and the wood slab with these QDs (right) are shown in Figure 2c (inset). The emission and absorption spectra of the QD wooden slab are provided in Figure 2c. Indeed, neither the luminescence spectrum nor the quantum yield was impacted upon incorporation of the QDs into the polymer or wood template. Quantum dots are known to be more resistant to bleaching than, e.g., organic dyes, and we found no changes in Si QDs optical properties when embedded in pure polymethyl methacrylate (PMMA) for months.[26]

Unlike previously described samples in Figure 1, which remain optically transparent after QD impregnation, the slab in Figure 2 is only partially transparent for the visible range and has a slightly brown color. While the Stokes shift is still significant for these relatively large Si QDs, their absorption markedly increases already in the green/blue spectral range (Figure 2c). For the samples of Si QDs with emission peak position closer to the visible range (red Si QDs in Figures 1 and 4) the wood transparency is largely unaffected by QD incorporation even at similar concentration levels. The large Stokes shift in that case makes smaller Si QDs absorption-free throughout most of the visible range.[26]

To evaluate the light scattering ability of this wood/polymer/QD hybrid the QD-based luminescence was collected at the sample edge by varying the excitation spot position. The schematic representation of this experiment is shown in **Figure 3**a (inset). The use of Si QDs with an appreciable apparent Stokes shift ensures the measured extinction is mainly contributed by scattering. It is known that light-emitting states of these Si QDs remain largely of indirect bandgap character[27] leading to long (≈µs) luminescence lifetimes[28] and strongly suppressed reabsorption at the emission wavelength.[15]

For an ideal slab with no scattering and reabsorption the collected intensity does not depend on the source position[29] (dotted line in Figure 3a). The fraction of light emitted from the slab edge is then defined only by the cone with a critical angle ≈42° (for the polymer/air refractive index contrast of ≈1.5/1). Above this angle the emitted light experiences total internal reflection inside the slab. In practice, inhomogeneities inside and on the slab surface lead to scattering outside of this cone. This is evident from the reference sample, where Si QDs were embedded into glass (blue line in Figure 3a). Here a fused silica slab was implanted with Si+ ions to create a nonstoichiometric glass and then annealed to form red emitting quantum dots.[30] The measured loss values for this sample are typical for real systems of QDs embedded in transparent matrices, such as glass or PMMA, which are of the same refractive index.[19] The losses can be minimized by more uniform and defect-free preparation of the host matrix and its surface, which is important for applications as large-area luminescent solar concentrators.

For quantum dots embedded in wood, the luminescence intensity reaching the edge becomes much lower. When the light propagation direction is parallel to the fibers (edge is perpendicular to fibers), the scattering losses amount to ≈3 dB cm^{-1} (black line in Figure 3a). In the case of perpendicular propagation relative to the fiber direction (edge is parallel to fibers) the losses become an order of magnitude larger, reaching ≈10 dB cm^{-1} (red line in Figure 3a). These direction-dependent losses clearly demonstrate the anisotropic structure of the wood template preserved in the QD nanocomposite. Figure 3b reveals this highly aligned hollow cell system of the wood. The cell wall thickness is around 1 µm, while the pore size ranges from around 10 to 60 µm with vessel pores being in the order of hundred microns. The fiber lengths are in the range from hundreds of micrometers up to a millimeter. When light propagates perpendicular to the fiber direction, more scattering centers are encountered at the cell wall-PMMA interfaces compared with propagation parallel to the fiber direction.

So only a small fraction of the emitted light reaches sample edges, yet there is negligible reabsorption in the sample. As a result, luminescence is mainly scattered out of plane, as explicitly shown in **Figure 4**a,b. Here we took photoluminescence photographs of the red Si QD glass and the red Si QD transparent wood samples under laser diode excitation (spot in the middle). The glass sample, as a planar waveguide, directs the light emission to the edges. In contrast, QD transparent wood displays a diffused luminescence in the whole chip, leading to a planar lighting instead. This is an attractive property in general

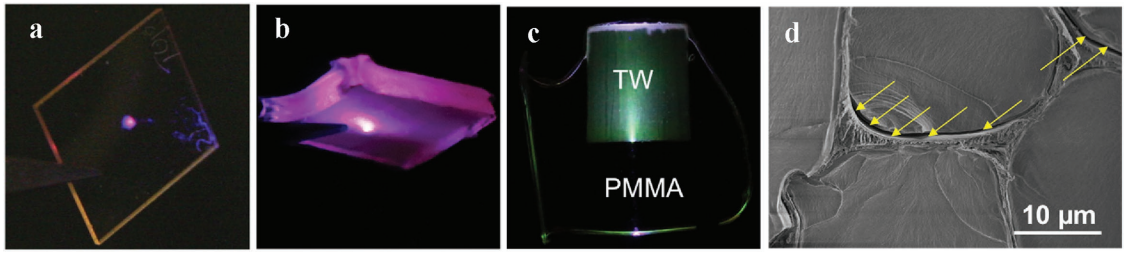

Figure 4. a) A photograph of Si QDs embedded in glass under 405 nm laser pumping (spot in the middle), demonstrating waveguiding of the emitted light to the edges and negligible scattering. b) A photograph of Si QD transparent wood under the same pumping, showing the diffused luminescence distributed over the whole piece. Due to the mixing of the scattered excitation blue light with the red emission it shows a pinkish appearance. c) A photograph of CdSe QD transparent wood integrated in a larger PMMA piece, where both wave-guiding and diffused luminescence coexist (excitation light is entering from the bottom center). d) A high-magnification SEM image of the Si QD transparent wood cross section, displaying interface gaps between wood cell walls and PMMA.

lighting, where light diffusers are often needed to generate spread, uniform illumination.

To demonstrate the possibility of incorporating different types of QDs in the transparent wood, CdSe QDs were also successfully embedded resulting in green luminescence. Figure 4c shows a photograph of CdSe QD transparent wood together with a PMMA envelope around it. When pumped from the PMMA edge (bottom center on the image) diffused luminescence in the CdSe QD transparent wood becomes visible. At the same time a fraction of the emission light is guided to the edges inside the PMMA layer. This proves that wood structured QD transparent composites provide a combination of a light diffuser with the conversion layer. A visibly better light propagation parallel to the fiber direction is also noticeable in this sample under the used in-plane excitation. Although CdSe QDs are known to exhibit some toxic effects,[31] they were selected here simply to show universality of the method for different QD material systems.

The origin of this diffused luminescence is mainly due to the small interface gaps between wood and PMMA, although optical inhomogeneities in cellulose fibers and in the PMMA also contribute. Though PMMA was fully infiltrated into the wood structure, interface gaps still exist in the composite due to nonoptimized chemical compatibility between cellulose and PMMA (Figure 4d). Additionally, PMMA shrinkage during polymerization contributes to the formation of interface gaps. Although these gaps are favorable when diffused scattering is desired (such as luminescent building or furniture and planar lighting), we could possibly further tune the scattering strength through wood surface modification. This can improve the interface quality and reduce scattering. Transparent wood with such haze control has potential applications ranging from planar lighting with highly diffused luminescent scattering to luminescent solar concentrators, where the waveguiding regime is favorable for light harvesting at the edges. We also note that a plywood configuration can be used to achieve more isotropic luminescence scattering. This nanocomposite material is expected to be less prone to degradation caused by moisture, microorganisms and UV radiation than original wood thanks to near-complete pore filling with PMMA, acting as an efficient barrier against liquid, and due to the removal of lignin, which is the main component subjected to UV-degradation in wood.

In conclusion, luminescent transparent wood combining optical and load-bearing functions was successfully fabricated by infiltration of a wood template with QD-rich MMA. No signs of optical degradation were detected upon this transition, indicating good compatibility of a transparent wood matrix for QD encapsulation. The wood structure introduced strong scattering, resulting in diffused luminescence from embedded quantum dots, which is advantageous for planar light sources and luminescent building construction elements or furniture. Surface modification of the wood cell wall will help to tune the light scattering properties of this new material, making it attractive for a wider range of applications.

Acknowledgements

Y.L. and S.Y. contributed equally to this work. The authors acknowledge financial support by Knut and Alice Wallenberg foundation through the Wallenberg Wood Science Center at KTH Royal Institute of Technology, and by the Swedish Research Council (VR) through an individual contract (VR 2015-04064) and ADOPT Center of Excellence. Regina Sinelnikov is acknowledged for providing some starting material.

Received: October 10, 2016
Revised: October 24, 2016
Published online: November 23, 2016

[1] Y. Shimizu, K. Sakano, Y. Noguchi, T. Moriguchi, US Patent 7,682,848 **2010**.
[2] H. V. Demir, S. Nizamoglu, T. Erdem, E. Mutlugun, N. Gaponik, A. Eychmueller, *Nano Today* **2011**, *6*, 632.
[3] S. Jun, J. Lee, E. Jang, *ACS Nano* **2013**, *7*, 1472.
[4] C.-C. Tu, J. H. Hoo, K. F. Boehringer, L. Y. Lin, G. Cao, *Opt. Express* **2014**, *22*, A276.
[5] L. Yang, Y. Liu, Y. L. Zhong, X. X. Jiang, B. Song, X. Y. Ji, Y. Y. Su, L. S. Liao, Y. He, *Appl. Phys. Lett.* **2015**, *106*, 173109.
[6] S. I. Chang, J. B. Yoon, H. K. Kim, J. J. Kim, B. K. Lee, D. H. Shin, *Opt. Lett.* **2006**, *31*, 3016.
[7] M. Y. Ghannam, A. A. Abouelsaood, J. F. Nijs, *Sol. Energy Mater. Sol. Cells* **2000**, *60*, 105.
[8] B. W. Lim, M. C. Suh, *Nanoscale* **2014**, *6*, 14446.
[9] C. C. Liu, S. H. Liu, K. C. Tien, M. H. Hsu, H. W. Chang, C. K. Chang, C. J. Yang, C. C. Wu, *Appl. Phys. Lett.* **2009**, *94*, 103302.
[10] G. Kim, *Eur. Polym. J.* **2005**, *41*, 1729.

[11] Y. Li, Q. Fu, S. Yu, M. Yan, L. Berglund, *Biomacromolecules* **2016**, *17*, 1358.
[12] J. Xue, F. Song, X.-w. Yin, X.-l. Wang, Y.-z. Wang, *ACS Appl. Mater. Interfaces* **2015**, *7*, 10076.
[13] S. Fink, *Holzforschung* **1992**, *46*, 403.
[14] M. W. Zhu, J. W. Song, T. Li, A. Gong, Y. B. Wang, J. Q. Dai, Y. G. Yao, W. Luo, D. Henderson, L. B. Hu, *Adv. Mater.* **2016**, *28*, 5181.
[15] I. Sychugov, F. Pevere, J. W. Luo, A. Zunger, J. Linnros, *Phys. Rev. B* **2016**, *93*, 161413(R).
[16] C. S. Erickson, L. R. Bradshaw, S. McDowall, J. D. Gilbertson, D. R. Gamelin, D. L. Patrick, *ACS Nano* **2014**, *8*, 3461.
[17] F. Meinardi, A. Colombo, K. A. Velizhanin, R. Simonutti, M. Lorenzon, L. Beverina, R. Viswanatha, V. I. Klimov, S. Brovelli, *Nat. Photonics* **2014**, *8*, 392.
[18] L. R. Bradshaw, K. E. Knowles, S. McDowall, D. R. Gamelin, *Nano Lett.* **2015**, *15*, 1315.
[19] F. Meinardi, H. McDaniel, F. Carulli, A. Colombo, K. A. Velizhanin, N. S. Makarov, R. Simonutti, V. I. Klimov, S. Brovelli, *Nat. Nanotechnol.* **2015**, *10*, 878.
[20] C. M. Hessel, E. J. Henderson, J. G. C. Veinot, *Chem. Mater.* **2006**, *18*, 6139.
[21] C. M. Hessel, D. Reid, M. G. Panthani, M. R. Rasch, B. W. Goodfellow, J. Wei, H. Fujii, V. Akhavan, B. A. Korgel, *Chem. Mater.* **2012**, *24*, 393.
[22] Z. Yang, C. M. Gonzalez, T. K. Purkait, M. Iqbal, A. Meldrum, J. G. C. Veinot, *Langmuir* **2015**, *31*, 10540.
[23] F. Sangghaleh, I. Sychugov, Z. Yang, J. G. C. Veinot, J. Linnros, *ACS Nano* **2015**, *9*, 7097.
[24] H. Yano, A. Hirose, P. J. Collins, Y. Yazaki, *J. Mater. Sci. Lett.* **2001**, *20*, 1125.
[25] F. Purcell-Milton, Y. K. Gun'ko, *J. Mater. Chem.* **2012**, *22*, 16687.
[26] A. Marinins, Z. Yang, H. Chen, J. Linnros, J. G. C. Veinot, S. Popov, I. Sychugov, *ACS Photonics* **2016**, *3*, 1575.
[27] B. Lee, J. W. Luo, N. Neale, M. Beard, D. Hiller, M. Zacharias, P. Stradins, A. Zunger, *Nano Lett.* **2016**, *16*, 1583.
[28] F. Sangghaleh, B. Bruhn, T. Schmidt, J. Linnros, *Nanotechnology* **2013**, *24*, 225204.
[29] G. Keil, *Nucl. Instrum. Meth.* **1970**, *89*, 111.
[30] I. Sychugov, N. Elfstrom, A. Hallen, J. Linnros, M. Qiu, *Opt. Lett.* **2007**, *32*, 1878.
[31] A. M. Derfus, W. C. W. Chan, S. N. Bhatia, *Nano Lett.* **2004**, *4*, 11.